Review

Biomimetic Aquatic Robots Based on Fluid-Driven Actuators: A Review

Kunlang Bu [1,2], Xiaobo Gong [1], Changli Yu [1] and Fang Xie [3,*]

1 School of Ocean Engineering, Harbin Institute of Technology, Weihai 264209, China;
   bukunlang2021@sjtu.edu.cn (K.B.); xiaobogong@hit.edu.cn (X.G.); yuchangli@hitwh.edu.cn (C.Y.)
2 University of Michigan–Shanghai Jiao Tong University Joint Institute, Shanghai Jiao Tong University,
   Shanghai 200240, China
3 School of Materials Science and Engineering, Harbin Institute of Technology, Weihai 264209, China
* Correspondence: fangxie@hit.edu.cn

Abstract: Biomimetic aquatic robots are a promising solution for marine applications such as internal pipe inspection, beach safety, and animal observation because of their strong manoeuvrability and low environmental damage. As the application field of robots has changed from a structured known environment to an unstructured and unknown territory, the disadvantage of the low efficiency of the propeller propulsion has become more crucial. Among the various actuation methods of biomimetic robots, many researchers have utilised fluid actuation as fluid is clean, environmentally friendly, and easy to obtain. This paper presents a literature review of the locomotion mode, actuation method, and typical works on fluid-driven bionic aquatic robots. The actuator and structural material selection is then discussed, followed by research direction and application prospects of fluid-driven bionic aquatic robots.

Keywords: biomimetic aquatic robot; fluid actuation; actuation method

1. Introduction

With the rapid development of technologies such as automated control, industrial manufacturing, and robot morphology, robots have played an increasingly important role in human society in recent decades. The application of robots has gradually extended from agricultural production, transportation, and aerospace to new areas closer to human life, such as in the fields of medicine, education, service, energy, and entertainment [1–4].

For marine engineering, robotic systems are being adapted to carry out complex missions in aqueous environments, including internal pipe inspection, beach safety, and animal observation [5–8]. Therefore, researchers have designed various underwater robots for aquatic missions, such as ROV and AUV, and these robots have aroused growing interest [9,10]. ROV and AUV are usually rigid robots, which use metal hinges and joints for connection and also have stiff material in the outer shell. For propulsion, these rigid robots often utilise screw propellers [11]. However, such propellers may produce much noise when they are functioning at high speed, which may disturb sea animals, and the rotating propeller may even cause harm to living creatures. At the same time, the propeller is unsuitable for operating in a complex and confined environment [12,13] as the blades can get entangled in underwater weeds or hit the seabed, causing damage to the propeller and resulting in mission failure. In recent years, with the strong demand for robots to operate in unstructured and unknown environments, the low efficiency of the propeller in complicated underwater areas has been magnified [13].

The soft body, excellent flexibility, and robust environmental adaptability of sea creatures provide new ideas for developing aquatic robots. Bionic aquatic robots are generally robots that imitate the structure or movement of marine animals. As a new type of robot,

biomimetic robots have the characteristics of high environmental adaptability, strong affability, and diverse functions [14–16]. They can be continuously deformed and have a high degree of freedom. Scientists draw inspiration from aquatic living creatures and use the latest robotic technology to design a series of underwater bionic robots [17–19].

Compared to propeller propulsion, the locomotion of aquatic animals has the characteristics of high manoeuvrability, high efficiency, low noise, good concealment, and little environmental disturbance. Therefore, they have better applications in various aquatic environments [20,21]. Unlike propeller-based robots, biomimetic robots have a variety of actuation methods, such as fluid actuation [22,23], smart material actuation (including shape memory alloy (SMA) [24–27], electroactive polymer (EAP) [28–31], piezoelectric materials (PZT) [32–37], chemical reaction actuation [38], biological hybrid actuation [39–41], magnetic field actuation [42–45], and a combination of these methods [46,47].

Fluid actuation has aroused the most interest among various actuation methods because of its advantages of being clean, environmentally friendly, and easy to achieve [48]. Fluid actuation deforms a specific structure through expansion and contraction, bending, and torsion by filling or withdrawing fluid. Fluid actuation can be divided into gas actuation and liquid actuation according to the actuation sources. Research on gas-driven robots started early [49]. Gas actuation plays an essential role in bionic aquatic robots due to its advantages of lightweight, low pollution, quick actuation, and reliable performance under substantial electromagnetic radiation interference [50,51]. The significant advantage of liquid actuation lies in its actuation sources. These include the surrounding water, which can be easily obtained and directly discharged into the ocean after use [52,53].

This review paper provides readers with an overall review of fluid-driven actuators and biomimetic aquatic robots using these actuators. In Section 2, four common locomotion modes are presented for biomimetic robots: undulation/oscillation, jet propulsion, walking, and rowing. Section 3 summarises fluid-driven actuators based on the actuation principle, along with their characteristics. Biomimetic aquatic robots using fluid-driven actuators are reviewed in Section 4. Section 5 provides suggestions for designing biomimetic robots, while challenges and prospects are presented in Section 6.

2. Classification of Locomotion Modes

The locomotion modes of aquatic animals can be divided into the following categories: undulation/oscillation motion, jet propulsion motion, rowing motion, and walking motion. The diagrams and core locomotion laws of these locomotion modes are shown in Table 1 [54–58]. It should be noted that some other motions, such as jumping, flying, and burrowing, exist in nature [16] but are rarely employed for biomimetic aquatic robots. Therefore, these motions are beyond the scope of this paper.

Table 1. Photographs, fundamental laws of various types of locomotion, and corresponding animals [54].

Locomotion Mode	Locomotion Law	Imitated Animal
Undulation/oscillation	$F = 0.5\rho A v^2 C_L$	Tuna, tortoise
Jet propulsion	$F_{input} = \frac{dmv_{inhale}}{dt}$ $F_{output} = \frac{dmv_{discharge}}{dt}$	Jellyfish
Rowing	$F = 0.5\rho S_{drag} v^2 C_d$	Frogs, ducks
Walking	Centre of mass $\in$ supporting surface	Sea crabs

Aquatic animals using undulatory/oscillatory motion achieve propulsion through periodic swings of the body or the wings (also known as body/caudal fin or median/paired fin [16]). According to the Bernoulli theorem, the pressure difference between the two sides of the water caused by the swing produces lift, and the resultant force of each lift forms a forward thrust. Familiar aquatic creatures that use undulatory/oscillation motion are

hairtail and eel (body swinging) and tuna, whale, and tortoise (wing swinging). It is worth noting that the reason why we do not distinguish between undulation and oscillation lies in their vague boundary. In [16], they pointed out that a wave passes through the whole body in undulation, while it only appears near the actuator in oscillation. However, Chu [59] believed that there is no clear distinction as the oscillatory motion can be derived from the undulatory movement with a shorter wavelength. Therefore, we combine the two modes in the following discussion.

Jet propulsion motion organisms first inhale water into the body and then discharge the water backwards, using the changes in the momentum of the inhaled water and the discharged water to achieve forward propulsion. Creatures that use jet propulsion are mainly jellyfish and cuttlefish.

Rowing motion animals are mainly frogs and ducks whose legs (or web and fins) function as oars. The locomotion process of the paddle can be divided into two stages: propulsion and recovery. The oars paddle backwards during the propulsion stage, and the water provides a forward counterforce to achieve propulsion. The oars are quickly retracted and kept as parallel to the incoming flow direction as possible to reduce resistance during recovery in the recovery stage.

Walking motion can be categorised into two types. The first type is multilegged crawling creatures, which is dominated by sea crabs and lobsters. These animals move similarly to multilegged creatures on land, using the friction between their feet and the ground to generate thrust. The second type is aquatic organisms, which are represented by anorectal organisms and plankton. They are often micro-organisms and mainly depend on viscous or capillary forces to swim forward [60].

3. Classification of Fluid Actuation Methods

Until recently, researchers have designed and manufactured a large number of fluid actuators. These actuators can be divided into linear actuators, bending actuators, and torsion actuators according to the deformation type. Depending on the actuation form, they can also be categorised into positive and negative pressure actuators. The actuation principle can be divided into McKibben-type actuator, Pneu-Net actuator, and vacuum buckling actuator. In this context, the actuation principle will be selected as the classification standard to discuss these actuators. As there are other fluid actuation methods and fluid hybrid actuators with application potential in biomimetic aquatic robots [61], they will also be described here.

3.1. McKibben-Type Actuator

American atomic physicist McKibben designed the first pneumatic artificial muscle in the 1950s [62]. A schematic diagram of McKibben muscle design is shown in Figure 1. The muscle is mainly composed of an elastic tube and a braiding jacket. After inflation at one end, the elastic tube expands. The direction of expansion is associated with the braiding angle. When the braiding angle is less than $54°44'$, the axial restraint of the braided mesh is dominant, and the muscle expands radially, which drives the actuator to contract axially. If it is higher than $54°44'$, the radial restraint is stronger, leading to the axial elongation motion of the muscle [63].

Further studies have been carried out based on the McKibben pneumatic actuator. In increasing deformation types, bending actuators, spiral actuators, and torsion actuators are designed by changing the structure and braiding angle of the outer constraint [64,65]. In terms of the structural design, the woven braiding can be embedded in the elastic tube, simplifying the structure and reducing the friction between the tube and the braided mesh [66]. In terms of material selection, researchers have replaced the woven mesh with a reinforced fibre structure [67,68], which improved the toughness of the system but reduced the corresponding deformation [49].
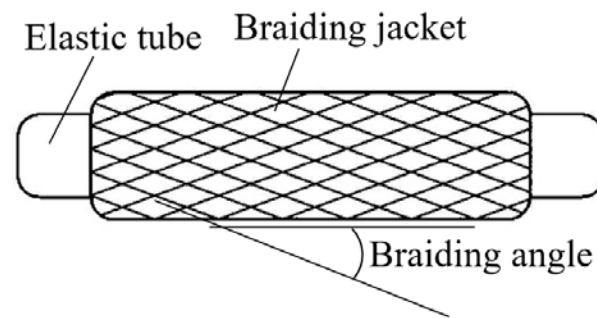
Figure 1. Schematic of McKibben-type pneumatic artificial muscle.

3.2. Pneu-Net Actuator

In 2011, Ilievski et al. [69] from Harvard University proposed and developed a new fluid elastic bending actuator called Pneu-Net. The top of the actuator is a stretched layer with better elasticity, and the bottom is an inelastic strain-limiting layer. Multiple internally connected cavities are set within the elastomer layer. When filled with gas, the cavities expand and squeeze the inner wall. Because of the difference in elasticity between the two layers, the structure bends toward the bottom layer.

The actuator is characterised by a linear array arrangement structure, which simplifies the manufacturing process but still has problems such as large gas consumption and slow driving speed [70]. To address these limitations, Mosadegh et al. [70] designed a gap between each chamber to reduce the influence of the repulsion between adjacent air chambers on the amount of deformation (Figure 2a). Meanwhile, the expansion layer gets thick while the inner wall becomes thinner, decreasing the ventilation volume and increasing the deformation angle. The improved actuator has also given rise to a lot of research studies, such as those investigating a pneumatic gripper that can grab fruits [71], robotic hand for packaging boxes [72], and general software pneumatic manipulator [73].
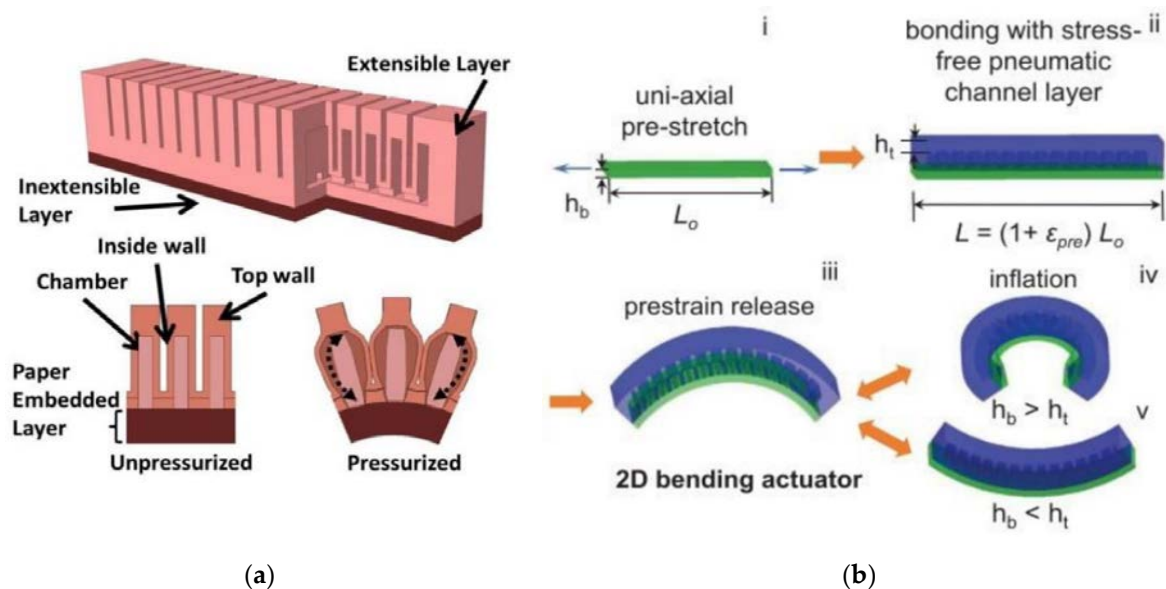

(**a**)   (**b**)

Figure 2. Pneu-Net actuator: (**a**) structural diagram of an optimised FEA [70], reproduced with permission from [70], 2014, John Wiley and Sons; (**b**) bistable precurved soft actuator [74], reproduced with permission from [74], 2020, John Wiley and Sons.

Pneu-Net also has various modifications. Suppose the actuator has been bent and deformed when the fluid is not filled, and another or several kinds of bending deformations are generated when inflated. In that case, the actuator can form two or more stable bending states. This bistable or multistable actuator also has excellent potential in soft robots [74,75].

Chi et al. [74] designed a prestretched 2D bending and 3D doming actuator (Figure 2b). This actuator comprises an elastic layer and a strain-limiting layer. The difference is that the elastic layer is stretched in advance to elongate during manufacture and then combined with an inextensible layer of the same length or diameter. After the tension constraint is released, the actuator bends to the side of the elastic layer. This type of actuator can realise various bistable structures and can be applied to grasping, crawling, adhesion, and underwater movement. Tang et al. [75] also developed a spine-inspired bistable soft actuator by implementing a spring as a 'spine'. The actuator amplifies the performance through the elastic potential energy of the spring, and the two bistable mechanisms can be applied to different occasions.

3.3. Vacuum-Powered Buckling Actuator

The vacuum-powered buckling actuator can be regarded as the inverse process of the positive pressure actuator. The elastic buckling structure consists of interconnected elastic air chambers and elastic beams. When negative pressure is applied, the air chamber shrinks, which causes the elastic beam to deform, and the actuator produces buckling. Yang et al. [76,77] from Harvard University first proposed a buckling actuator and investigated the design and performance of the actuator (Figure 3). The designed bending actuator can grab a piece of chalk, while the linear actuator can lift objects weighing 500 g. Jiao et al. [78] combined multiple vacuum actuators to form various linear and torsional motions. The actuator has also been applied to pipe-crawling robots and four-wheeled robots. Moreover, Ainla et al. [79] used the vacuum buckling actuator for liquid stirring.
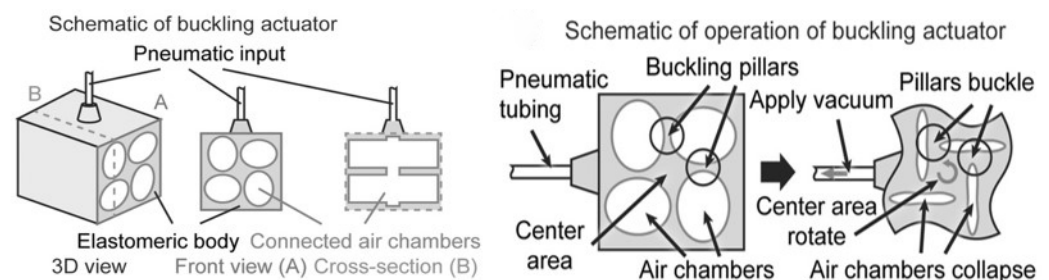

Figure 3. A Vacuum-powered buckling actuator [76], reproduced with permission from [76], 2015, John Wiley and Sons.

Vacuum buckling actuators are often combined with origami structures. The origami skeleton acts as an elastic beam, and the cavity between the skeleton and the outer skin is equivalent to an elastic air chamber. Lee and Rodrigue [80] used metal as the origami skeleton, significantly improving the performance. Under a vacuum of 10 kPa, it can reach a deformation rate of 85% under a load of 8 kg.

3.4. Combustion Actuation

Combustion actuation generates thrust through high-temperature and high-pressure gas produced by chemical reactions. Shepherd et al. [81] designed a jumping robot powered by combustion, as shown in Figure 4. The robot consists of a combustion chamber and three pneumatic bending drives at 120° to each other. Methane and oxygen are filled into the combustion chamber and ignited by an electric spark. With a body length of 130 mm, the robot can jump to a position 30 times its height in 0.2 s, and the jumping speed is ~3.6 m/s. Bartlett et al. [82] also designed a soft jumping robot powered by combustion. The body expands and squeezes the ground, and the reaction force from the ground makes the robot jump upwards after mixing and burning reactants.
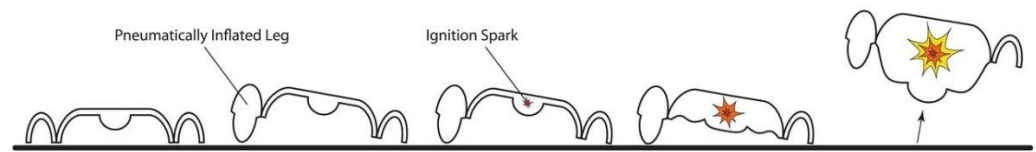
Figure 4. Untethered jumping robot powered by combustion [82], reproduced with permission from [82], 2015, American Association for the Advancement of Science.

4. Biomimetic Aquatic Robot Using Fluid Actuation

Table 2 summarises robots using different fluid actuation methods. In brief, the aquatic robots are listed according to the actuation method.

4.1. McKibben-Type Actuated Aquatic Robots

4.1.1. Undulation/Oscillation Motion

A manta ray robotic fish was developed by Suzumori et al. [83]. Here, two McKibben actuators with reinforcing fibre are arranged on the two wings of the manta ray robot, and the bending motion of the actuators makes the wings oscillate to achieve propulsion. Feng et al. [84] designed an eel-like robot with a maximum swimming speed of 5.45 cm/s. Cai et al. [85] designed the underwater flapping-wing robot Robo-ray II (Figure 5a). The robot has two built-in McKibben artificial muscles. It exhibits a faster swimming speed with increased flapping frequency and amplitude, and the maximum swimming speed is 160 mm/s when the air pressure is 0.4 MPa and the flapping frequency is 1.2 Hz.

A carangiform underwater robot actuated by flexible matrix composite was developed at Virginia Polytechnic Institute and State University [86,87]. Here, 12 linear actuators are arranged in the back half of the fish, and the combined actuation of different actuators causes the tail fin to produce oscillating motion. Stable thrust output was found to be 1 Hz, and a maximum speed of 0.9 m/s can be obtained at this frequency.

(**a**)   (**b**)
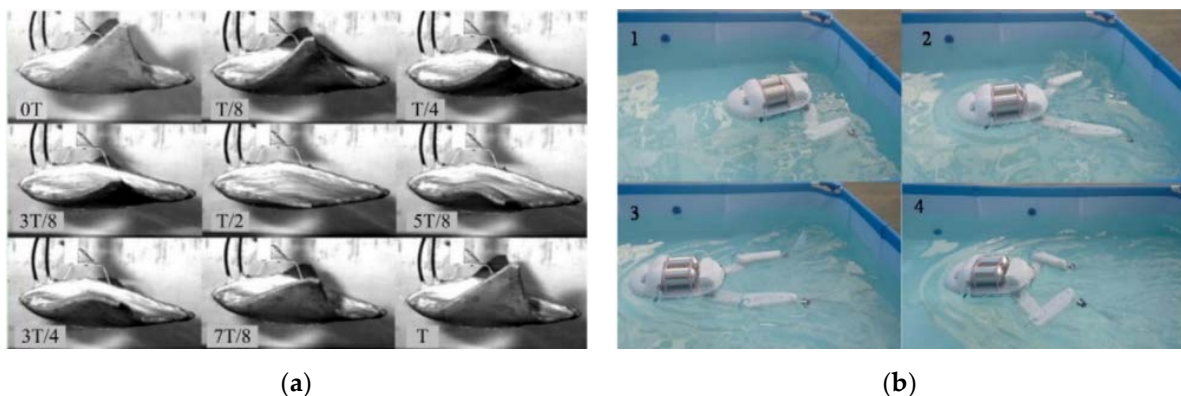
Figure 5. McKibben-type aquatic robots: (**a**) the undulation/oscillation bionic aquatic robot Robo-ray II [85], reproduced with permission from [85], 2010, Springer Nature; (**b**) frog-inspired rowing robot [88].

4.1.2. Rowing Motion

A frog-inspired robot (Figure 5b) was developed, which can achieve forward swimming and turning motions by imitating the movement of the hind limbs of a black-spotted frog [88]. Each joint of the frog has two McKibben muscles mounted in an antagonistic way to control the joint stiffness and position. Two muscles are connected by a crank. When one side of the McKibben muscle is charged, the crank rotates clockwise or anticlockwise, actuating the whole joint.

Table 2. Fluid-driven biomimetic robots and their size, weight, and operation speed (N/A means no available data).

Robot Name	Actuator	Locomotion Mode	Size (mm)	Weight (kg)	Speed (cm/s)
Manta swimming robot [83]	McKibben	Undulation/oscillation	170 × 150	N/A	10
Robo-ray II [85]	McKibben	Undulation/oscillation	320 × 560	3.8	8–16
Tethered-free streaming fish [86,87]	McKibben	Undulation/oscillation	580 × 190 × 140	~5	90
Eel-inspired soft robot [84]	McKibben	Undulation/oscillation	26 (diameter) × 240 (for actuator)	N/A	2.88 (average), 5.45 (maximum)
Frog-inspired robot [88]	McKibben	Rowing	590 × 340	12	N/A
Soft underwater walking robot [52]	McKibben	Walking	N/A	0.356	1.5
Robotic tuna [89]	Pneu-Net	Undulation/oscillation	2400 × 1000	173.1	125
Autonomous soft robotic fish [22]	Pneu-Net	Undulation/oscillation	339 × 51	N/A	15
Robotic fish [55]	Pneu-Net	Undulation/oscillation	450 × 190 × 130	1.65	10
SoFi [53]	Pneu-Net	Undulation/oscillation	470 × 230 × 180	1.6	3.2
Eel-inspired robot [90]	Pneu-Net	Undulation/oscillation	255 × 45	N/A	1.25
High-speed swimmer [75]	Pneu-Net	Undulation/oscillation	150	0.091	~11.7
Soft flapping-wing robot [91]	Pneu-Net	Undulation/oscillation	150	0.0028	56.1
Soft robotic jellyfish [48]	Pneu-Net	Jet propulsion	210	N/A	N/A
FludoJelly [56]	Pneu-Net	Jet propulsion	220	~0.6	16
Bistable jellyfish-like soft robot [74]	Pneu-Net	Jet propulsion	~200	N/A	5.33
Robotic dog [92]	Pneu-Net	Rowing	700	2.3	2.1
Frog-inspired robot [57,93]	Pneu-Net	Rowing	175 × 100 × 60	1.29	7.5
Rowing arthrobot [94]	Pneu-Net	Rowing	500	0.025	N/A
Swimming robot [95]	Vacuum buckling	Jet propulsion	220	N/A	5.53
A rowing swimmer [76]	Vacuum buckling	Rowing	~50	N/A	~2.4

4.1.3. Walking Motion

Developed at the University of California, an underwater quadruped robot consists of four soft hydraulic legs and a morphing body attached to a rigid frame [52]. The weight of the robot underwater is only 2.87 N. When walking with the flow, the speed when the front and rear skins are expanded is 16% higher than when they are not. However, when walking against the current, the morphing body filled with water will be pushed in the opposite direction by the water flow, while the flat body still has a movement speed of 0.09 mm/s.

4.2. Pneu-Net Actuated Robot

4.2.1. Undulation/Oscillation Motion

The first bionic robot to use a principle similar to the fluid elastomer actuator was the underwater bionic robot Robotic Tuna, which was developed by Massachu-setts Institute of Technology (MIT) in 2002 [89]. The left and right sides of the tail of the robot are separated to provide propulsion. Each side is composed of multiple flexible fins with a cavity between two adjacent fins. If cavities on the left side are filled with fluid, the left half expands and the tail is bent to the right and vice versa. RoboTuna has a maximum movement speed of 1.25 m/s at 1 Hz. It also achieves a top instantaneous turning speed of 75°/s and a turning radius of about two body lengths. Inspired by Robotic Tuna, Marchese and Katzschmann [23,54,56] made a series of improvements (Figure 6a,b).

A robotic fish inspired by lionfish was designed at Cornell University [23]. Here, a zinc–iodine battery cell is fitted inside the robotic fish. On the one hand, the battery cell

can supply power to the electronic equipment. On the other hand, the electrolyte inside the cell can be circulated and pumped into the tail actuator cell to achieve forward swimming.

An eel-like robot [90] with a body length of 255 mm and height of 45 mm was developed with two elastic bending actuators connected in series. The elongated body fish robot undulates its body to create thrust force for swimming forward. The maximum propulsion force is 0.297 mN at 3.3 Hz. The modified Pneu-Net in Section 3.2 also performs well in aquatic bionic robots. The biomimetic fish is actuated by a spine-inspired bistable actuator [75] with a body length of ~150 mm and a mass of ~51 g. Its swimming speed can reach up to 0.78 body length/s actuated at 160 kPa with a swing frequency of 1.3 Hz, which is better than a soft actuator and hybrid soft actuator under the same conditions. Moreover, Chi et al. [91] incorporated the nature of flying and swimming and designed a lightweight (2.8 g) flapping-wing robot. A precurved Pneu-Net actuator functioned as the fish body, resulting in a bending motion of the passive wing. When inflated, the actuator bends in another direction, causing flapping of the wing. The robotic fish has both high linear swimming speed and turning speed.

4.2.2. Jet Propulsion Motion

A jet propulsion aquatic robot inspired by moon jellyfish was developed at the Naval Surface Warfare Center, Carderock Division [48]. The eight actuators of the bionic jellyfish are evenly distributed along the circumference, and two pumps supply water to the four actuators on the left and the right. The flexible structure enables the bionic robot to pass through a narrow hole (160 mm) slightly smaller than its body diameter (210 mm). FludoJelly also utilises eight evenly distributed pneumatic actuators [56]. The robot can move upstream at a speed of 160 mm/s under the pressure of 483 kPa and a load of 100 g.

Chi [74] applied a 3D dome actuator with a 40% prestretch rate to the jellyfish robot (Figure 6c). Upon pressurisation, the doming actuator deforms quickly, forming a deep dome shape to push the enclosed water and propel itself forward. The robot can achieve an average swimming speed of 53.3 mm/s under a frequency of 0.67 Hz and pneumatic pressure of 30 kPa.

(**a**)　　　　　　　　　　　　　　　　　　　(**b**)

(**c**)　　　　　　　　　　　　　　　　　　　(**d**)
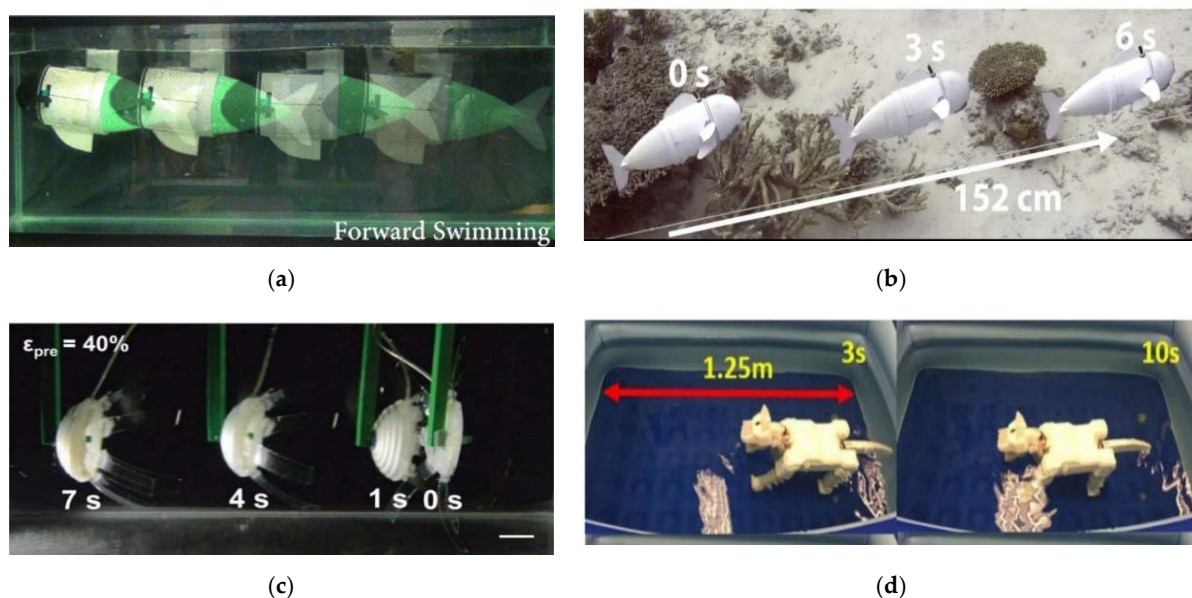
Figure 6. Aquatic robots actuated by Pneu-Net. (**a**) 3D diving robot [55], reproduced with permission from [55], 2016, Springer Nature; (**b**) acoustically controlled soft robotic fish [53], reproduced with permission from [53], 2018, American Association for the Advancement of Science; (**c**) fast swimming bistable jellyfish robot [74], reproduced with permission from [74], 2020, John Wiley and Sons; (**d**) bioinspired robotic padding dog [92], reproduced with permission from [92], 2019, IOP Publishing Ltd.

The University of Hong Kong developed a dog-paddling robot (Figure 6d) [92]. The legs of the robot use precharged pneumatic (PCP) actuators. The PCP actuator consists of a precharged Pneu-Net and a tendon. One end of the tendon is connected to the tip of Pneu-Net, and the other end is controlled by a motor. When the motor pulls the tendon, the precharged bending Pneu-Net becomes straight. The actuator bends again after releasing the tendon. The generation and release of the pulling force obtains a bending motion.

A biomimetic frog robot was developed at Harbin Institute of Technology [57]. The robot achieves an average movement speed of 75 mm/s. Furthermore, the robotic frog can turn 90° at a rate of 15 °/s with a turning radius of 0.2 m. The author made improvements in his later work [93], with the identical actuators added to the shoulder and elbow joints of the forelimbs. The average movement speed increased to 100 mm/s, and the turning radius was reduced to 0.15 m.

A lightweight robot inspired by arthropods was designed by Nemiroski [94]. The robot is made up of multiple legs with pneumatic tubes inside the legs. In each leg, some joints are fabricated to connect different leg parts. An elastomeric tendon connects one side of the joint. When inflated, the tube expands towards the tendon, resulting in the bending of the leg. The six-leg arthrobot is lightweight (2.5 g) and can row on water.

4.3. Vacuum-Powered Buckling Actuator

Cheng et al. [95] designed a jellyfish robot (Figure 7) actuated by a novel cylindrical soft vacuum actuator (CSVA). When applying vacuum, the bottom layer in the jellyfish body is sucked into the internal chamber, breathing in water. Then, water is expelled out when the vacuum disappears, leading to the momentum of the robotic fish. The maximum swimming speed of the robot reaches 5.53 cm/s when the frequency of flapping motion is 0.6 Hz.
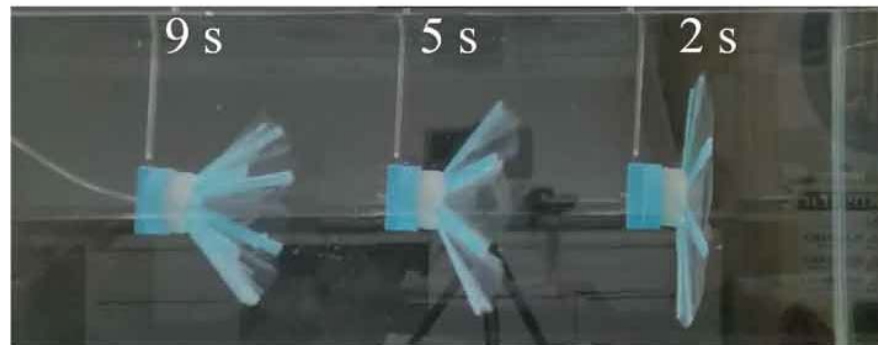

Figure 7. Aquatic robots actuated by vacuum buckling [95], reproduced with permission from [95], 2021, IOP Publishing Ltd.

A rowing robot propelled by a vacuum-powered buckling actuator was developed at Harvard University [76]. The robot consists of a buckling actuator, passive leg (connected to the actuator), and paddle. When negative pressure is applied to make the actuator contract, the leg rotates counter-clockwise, and the lightweight paddle moves clockwise because of the water flow.

4.4. Other Fluid Actuation Methods

Keithly et al. [96] designed a cephalopod-inspired jet propulsion engine (Figure 8a). The robot uses high energy density methane combustion to expand a silicone bladder and accelerate water into a hydrojet to generate propulsion. Another fish developed in [97] can use the thrust generated by the combustion to escape from water multiple times.

(**a**)   (**b**)
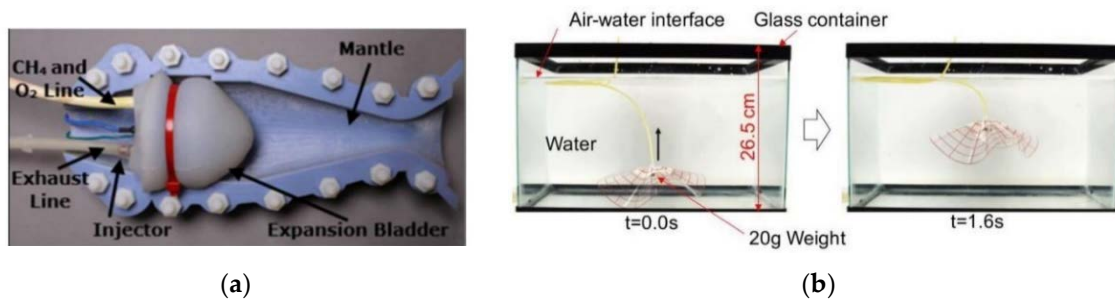
Figure 8. Other fluid-driven aquatic robots: (**a**) A cephalopod-inspired combustion engine for jet propulsion fish [96], reproduced with permission from [96], 2018, Elsevier; (**b**) light-weight jellyfish animal [98], reproduced with permission from [98], 2021, PNAS.

Nagarkar et al. [98] designed a lightweight jellyfish robot actuated by the buckling sheet actuator (Figure 8b). The buckling sheet actuator is based on a circular transparent sheet of polycellulose acetate. A thin circular nylon film is then attached to the centre of the sheet using double-sided tape to form a bladder. The robot can swim vertically from the bottom of a 26.5 cm pool to the surface in 2.5 s with an additional mass of 20 g.

5. Discussion on Biomimetic Aquatic Robot Design

Based on the above works, we propose a roadmap for designing biomimetic aquatic robots, as shown in Figure 9. Each step of the roadmap is discussed in detail in the following sections.
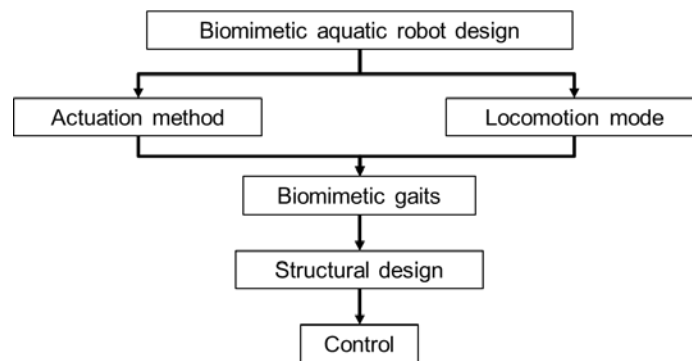
Figure 9. Roadmap for biomimetic robot design.

5.1. Actuation Method

The actuation method selection and the locomotion mode in Section 5.2 are the first steps for biomimetic aquatic robot design. Different actuation methods and their driving pressure, frequency, and characteristics are shown in Table 3. It is worth noting that selecting the actuation fluid (gas or liquid) is also essential in determining the actuation method. Therefore, the selection of working fluid is discussed in the following section.

5.1.1. McKibben Actuator

The McKibben actuator has a simple structure. The simplest McKibben muscle only contains braided mesh and elastic tube, which is easy to fabricate by hand. The muscle can withstand high atmospheric pressure (up to 0.6 MPa) [65]. Thus, it is less dangerous when the gas source is out of control. However, the actuator has internal friction between the tube and the mesh, leading to hysteresis of the actuator and making precise control difficult [49,62]. Moreover, the twisting of braiding mesh makes McKibben muscle difficult for large-scale manufacturing. Although the McKibben muscle can achieve bending, twisting, winding, and other forms of motion by changing the geometric arrangement of the braiding

mesh [68,99,100], the McKibben muscle is more often used for linear deformation [85,88]. Bending motion can be obtained by designing passive structures or control methods.

Table 3. Description of various actuation methods and their working pressure, frequency, advantages, and disadvantages.

Actuation Methods	Description	Working Pressure (MPa)	Frequency (Hz)	Advantages and Disadvantages
McKibben muscle	● Composed of inserted elastic tube and restricting outer shell ● Expansion direction related to the geometric arrangement of the restricting shell	0.15 to 0.6 [83,88]	0.4 to 2 [84]	● Simple structure and manual processing ● Withstands high air pressure ● High friction loss ● Difficult for mass manufacturing
Pneu-Net	● Consisting of an extensible layer, inextensible layer, and air chamber ● The difference in elastic modulus of the two layers leads to deformation	0.01 to 0.09 [57,75]	0.8 to 5.2 [74,90]	● Simple structure and easy manufacturing ● Low required pressure for large deformation ● Only bending motion
Vacuum buckling	● Composed of an interconnected chamber and elastic beam ● Negative pressure causes contracted connected chambers, leading to bend and buckle	−0.002 to −0.1 [76,95]	0.6 to 2 [76,95]	● Compact structure ● Limited propulsion force ● Requires vacuum pump
Combustion	● High-temperature and high-pressure gas generated by chemical reaction to produce momentum	~0.1 [101]	<1 [102]	● High propulsion force ● Limited frequency due to gas circulating ● Potential environmental damage

5.1.2. Pneu-Net Actuator

Pneu-Net does not require high driving pressure, with only 100 kPa or even <100 kPa being sufficient [71,75,76]. Although the air pressure is not so high, the bending amplitude can be significant with high actuation frequency because the deformation mechanism is based on the modulus difference between the upper and lower layers [69]. Pneu-Net can be fabricated by 3D printing and casting moulding [69]. The previously mentioned biomimetic aquatic robots require bending motion in most locomotion modes, such as body swinging in undulation motion and leg bending for walking. Pneu-Net is a bending actuator by nature, meaning that no additional design is needed to transform the linear motion into bending motion. Due to its low driving pressure, uncomplicated design, and bending nature, Pneu-Net is more favoured by researchers in designing biomimetic robots.

5.1.3. Vacuum Buckling Actuator

The vacuum buckling actuator does not require a large working space as it shrinks when applying vacuum. Thus, it has good application potential because the narrow space restricts the deformation of the actuator. Moreover, buckling actuators do not suffer from the explosion problem due to excessive inflation pressure [76]. However, a vacuum pump is needed. Moreover, because the output force of the actuator is correlated with the pressure difference, its output thrust is relatively small in a standard pressure environment (the maximum pressure difference is the residual pressure of the air chamber) [76].

5.1.4. Combustion Actuation

Combustion actuation can rapidly produce high-temperature and high-pressure gas to produce high-power locomotion through chemical reactions [81]. However, the chemical reaction has high instability, and the combustion actuation efficiency is relatively low. Moreover, because the next propulsion occurs only when the previous reaction is finished and the products have been released, the actuation frequency of combustion is relatively low (no more than 1 Hz [102]). Therefore, combustion actuation is mainly used in rapid movements, such as jumping and accelerating [81,97].

5.1.5. Working Fluid Selection

According to the actuation source, fluid actuation can be divided into gas actuation and liquid actuation. The commonly used actuation gases are compressed air [85], CO_2 [22], and combustion gas products [82]. The actuation liquid can be water [52,53] and electrolytes [23].Gas has high compressibility and low density, so it is convenient for storage, and the stored gas does not add too much weight. Besides, the lightweight allows the gas actuation system to have a faster response speed. However, the gas supply for aquatic robots with pneumatic actuators usually comes from an external gas pipe [75] or portable gas cylinder [22,88]. A robot with an outer air pipe has its navigation range limited by the air pipe. In addition, using a portable air tank may reduce its endurance. The light mass of the gas also causes its output force to be less than that of liquid actuation under the same conditions [103], and the asymmetric gas actuation may also lead to a fluctuating buoyancy centre, affecting the stability of locomotion [55].

The liquid is denser and has poor compressibility, which allows the liquid actuation system to have a greater output force. In particular, if the underwater robot uses water as the actuation fluid, the actuation source will be easy to obtain. For example, in the work of Frame et al. [48], the surrounding water was pumped to inflate the bending actuator and discharged to the environment. This open-loop control is simple and effective. However, liquid pumps are generally heavier and consume more energy than gas pumps, which reduces the locomotion efficiency of the robot, and the actuation speed tends to be relatively slow.

5.2. Locomotion Modes

Each of the four locomotion modes has its specific characteristics. A detailed description of various locomotion modes is shown in Table 1. The undulation/oscillation type has an overall unified movement, which is helpful for modular design and manufacturing [104–106]. For example, one easy way to obtain undulation/oscillation is to implement a bending actuator in the fishtail. The undulation/oscillation motion is achieved through periodic bending of the actuator [75]. However, this mode has difficulty dealing with pure upward/downward swimming, and other structures such as dive planes [55] are needed to achieve sinking or floating.

Jet propulsion can produce various locomotion attitudes [26], such as linear swimming and floating/sinking. However, as jet propulsion has to expel water to the outer environment, sufficient propulsion force is required for the jet propulsion cycle [107].

The rowing motion has high efficiency, but there are still considerable difficulties in gait design and control. Moreover, rowing motion fails when it comes to underwater locomotion [88].

Walking animals can imitate the design technology of terrestrial robots, and walking is the only choice when robots are required to move on the seabed. However, the walking speed is low as walking does not utilise the water for propulsion [52].

5.3. Biomimetic Gaits

When the locomotion mode and the actuator have been chosen, biomimetic gaits should be designed. One example of rowing gait design is shown in Figure 10 [76]. In gait

design, the predicted motion of actuated and unactuated robots has to be ensured so that the locomotion of aquatic robot can be achieved.
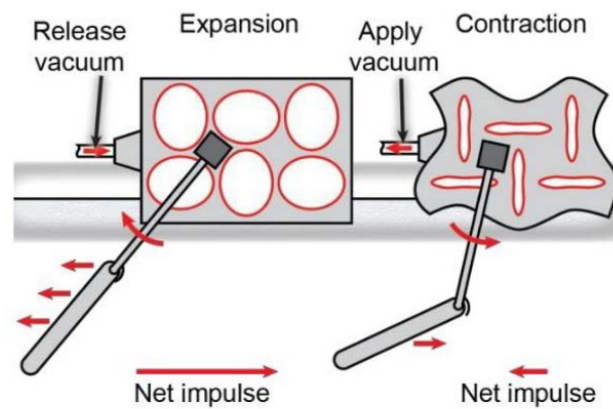
Figure 10. One example of biomimetic gait design [76], reproduced with permission from [76], 2015, John Wiley and Sons.

5.4. Structural Design

The main focus of the structural design is the material selection for the outer shell. Structural materials are usually divided into rigid materials and soft materials. Rigid materials mainly include metal (aluminium and stainless steel), plastics (PVC and polystyrene), and composite materials (carbon fibre). Soft materials are mostly latex and some rubber materials. Rigid materials are easy to manufacture, have good structural strength, and can withstand large impacts [96]. However, they have poor flexibility and are difficult to match with many soft actuators. Therefore, rigid shells are usually used for motor-driven robots. Soft materials show great advantages in combination with fluid actuators. For example, soft wings can produce good locomotion using fluid actuators [85]. With the maturity of various additive manufacturing and 3D printing techniques, the manufacturing of soft materials has become more accessible. Consequently, more researchers have begun to work on robots with soft materials.

5.5. Control

The control part of the biomimetic aquatic robot centres on working fluid control. As the pressure and flow rate determine the deformation of the actuator, theoretical model or simulation methods should be utilised to verify the appropriate parameters for locomotion. The control methods can be divided into two ways for actual locomotion control. One way is to directly control the pressure of the actuator through a pressure sensor, thereby controlling the movement of the robot. The other is to utilise deformation or motion sensors to feed back the motion or deformation information of the robot and control the intake and exhaust of the actuator by motion sensors [99,108]. When using a pressure sensor, the whole system simplifies, but the accuracy is not high. Implementing deformation or motion sensors may obtain precise control of the robot locomotion while adding complexity to the system design. Both advantages and disadvantages need to be considered when choosing control methods.

6. Challenges and Future Prospects

Bionic aquatic robots are constantly being optimised to adapt to more complex tasks. It will complete practical underwater tasks, such as underwater photography, sonar detection, monitoring and warning, underwater equipment repair, and underwater biological capture. However, there remain enormous challenges for biomimetic robots to fulfil these tasks. Future research may focus on the following aspects:

- **Fluid source and transportation**. At present, most fluid-driven biomimetic aquatic robots usually use external tubes for fluid supply [94,95]. Although external sources

are suitable for tasks requiring low mobility, they will significantly limit the scope of operation and affect workability. Some works contain pumps or gas tanks with the robot for fluid source and transportation [55,88], but they increase the weight of the robot and flexibility is reduced. Therefore, the trade-off effect between mobility and flexibility should be considered.

- **System reliability of the fluid actuating system**. Fluid-driven biomimetic robots often use multiple actuators to form a connected fluid actuation network to amplify the propulsion force [87]. If an actuator is damaged, the whole system may fail and get lost in the environment. Therefore, it is necessary to establish a corresponding antidamage structure to prevent failure or design a damage management system so that the whole robotic system keeps working or calls for help;
- **Bionic design from various perspectives**. Most biomimetic robots are mainly concentrated on structural and locomotion imitation. With the development of multifunctional soft robots, more results have been obtained on functional imitation, such as fast escape from the dangerous region [22,97]. Based on artificial neural networks, machine learning, visual recognition, and other technologies, the characteristics of biomimetic robots will be closer to natural creatures.
- **Deep-sea biomimetic robots**. Currently, the workspace of aquatic robots is still limited to the water surface or shallow water. However, the desire to explore the ocean calls for more robots that can enter the deep sea. Traditional ROVs or AUVs produce much noise due to screw propellers, which may scare away underwater animals. Biomimetic robots have the potential for better underwater observation, and some aquatic bionic robots have entered deep into the sea, such as in the Mariana Trench [30]. More study needs to be conducted on deep-sea biomimetic robots.
- **Human–machine cooperation control**. Robots are often inseparable from the management and supervision of humans in practice. However, an operator can only control one robot, which requires high human resources and limited operational efficiency. The demand for multiple robots working together will become more and more prominent in the future, such as joint salvage. How to realise the collaborative control between people and robots, or robots themselves, and break the one-to-one pattern of human control will also become a research hotspot in biomimetic aquatic robots.

Author Contributions: Conceptualization, X.G. and F.X.; methodology, X.G.; formal analysis, K.B. and F.X.; writing—original draft preparation, K.B.; writing—review and editing, X.G. and C.Y.; visualization, K.B. All authors have read and agreed to the published version of the manuscript.

Conflicts of Interest: The authors declare no conflict of interest.

References

1. Babel, F.; Vogt, A.; Hock, P.; Kraus, J.; Angerer, F.; Seufert, T.; Baumann, M. Step Aside! VR-Based Evaluation of Adaptive Robot Conflict Resolution Strategies for Domestic Service Robots. *Int. J. Soc. Robot.* **2022**, *14*, 1–22. [CrossRef]
2. Montobbio, F.; Staccioli, J.; Virgillito, M.E.; Vivarelli, M. Robots and the origin of their labour-saving impact. *Technol. Forecast. Soc. Chang.* **2022**, *174*, 121122. [CrossRef]
3. Wang, E.-Z.; Lee, C.-C.; Li, Y. Assessing the impact of industrial robots on manufacturing energy intensity in 38 countries. *Energy Econ.* **2022**, *105*, 105748. [CrossRef]
4. Wang, G.; Phan, T.V.; Li, S.; Wang, J.; Peng, Y.; Chen, G.; Qu, J.; Goldman, D.I.; Levin, S.A.; Pienta, K.; et al. Robots as models of evolving systems. *Proc. Natl. Acad. Sci. USA* **2022**, *119*, e2120019119. [CrossRef]
5. Yu, K.L.; Kastein, H.; Peterson, T.; Clark, C.; White, C.; Lowe, C. Using time of flight distance calculations for tagged shark localization witn an AUV. In Proceedings of the 18th International Symposium on Unmanned Untethered Submersible Technology: UUST 2013, Portsmouth, NH, USA, 11–14 August 2013; pp. 171–181.
6. Tan, X.B. Autonomous Robotic Fish as Mobile Sensor Platforms: Challenges and Potential Solutions. *Mar. Technol. Soc. J.* **2011**, *45*, 31–40. [CrossRef]

7. Christianson, C.; Bayag, C.; Li, G.; Jadhav, S.; Giri, A.; Agba, C.; Li, T.; Tolley, M.T. Jellyfish-Inspired Soft Robot Driven by Fluid Electrode Dielectric Organic Robotic Actuators. *Front. Robot. AI* **2019**, *126*. [CrossRef]

8. Conte, J.; Modarres-Sadeghi, Y.; Watts, M.N.; Hover, F.S.; Triantafyllou, M.S. A fast-starting mechanical fish that accelerates at 40 m s^{-2}. *Bioinspir. Biomim.* **2010**, *5*, 035004. [CrossRef]

9. Colgate, J.E.; Lynch, K.M. Mechanics and control of swimming: A review. *IEEE J. Ocean. Eng.* **2004**, *29*, 660–673. [CrossRef]

10. Youssef, S.M.; Soliman, M.; Saleh, M.A.; Mousa, M.A.; Elsamanty, M.; Radwan, A.G. Underwater Soft Robotics: A Review of Bioinspiration in Design, Actuation, Modeling, and Control. *Micromachines* **2022**, *13*, 110. [CrossRef]

11. Bogue, R. Underwater robots: A review of technologies and applications. *Ind. Robot.* **2015**, *42*, 186–191. [CrossRef]

12. Wang, Z.; He, Q.; Cai, S. Artificial Muscles for Underwater Soft Robotic System. In *Bioinspired Sensing, Actuation, and Control in Underwater Soft Robotic Systems*; Paley, D.A., Wereley, N.M., Eds.; Springer International Publishing: Berlin/Heidelberg, Germany, 2021; pp. 71–97.

13. Castaño, M.L.; Tan, X. Model Predictive Control-Based Path-Following for Tail-Actuated Robotic Fish. *J. Dyn. Syst. Meas. Control.* **2019**, *141*, 11. [CrossRef]

14. Salazar, R.; Campos, A.; Fuentes, V.; Abdelkefi, A. A review on the modeling, materials, and actuators of aquatic unmanned vehicles. *Ocean Eng.* **2019**, *172*, 257–285. [CrossRef]

15. Rich, S.I.; Wood, R.J.; Majidi, C. Untethered soft robotics. *Nat. Electron.* **2018**, *1*, 102–112. [CrossRef]

16. Sfakiotakis, M.; Lane, D.M.; Davies, J.B.C. Review of fish swimming modes for aquatic locomotion. *IEEE J. Ocean. Eng.* **1999**, *24*, 237–252. [CrossRef]

17. Palmisano, J.; Geder, J.; Rarriairiurti, R.; Liu, K.J.; Cohen, J.J.; Mengesha, T.; Naciri, J.; Sandberg, W.; Ratna, B. *Design, Development, and Testing of Flapping Fins with Actively Controlled Curvature for an Unmanned Underwater Vehicle*; Springer: Tokyo, Japan, 2008; pp. 283–294.

18. Guo, J. Optimal measurement strategies for target tracking by a biomimetic underwater vehicle. *Ocean Eng.* **2008**, *35*, 473–483. [CrossRef]

19. Hou, Y.L.; Hu, X.Z.; Zeng, D.X.; Zhou, Y.L. Biomimetic Shoulder Complex Based on 3-PSS/S Spherical Parallel Mechanism. *Chin. J. Mech. Eng.* **2015**, *28*, 29–37. [CrossRef]

20. Fish, F.E.; Kocak, D.M. Biomimetics and Marine Technology: An Introduction. *Mar. Technol. Soc. J.* **2011**, *45*, 8–13. [CrossRef]

21. Villanueva, A.; Smith, C.; Priya, S. A biomimetic robotic jellyfish (Robojelly) actuated by shape memory alloy composite actuators. *Bioinspir. Biomim.* **2011**, *6*, 036004. [CrossRef]

22. Marchese, A.D.; Onal, C.D.; Rus, D. Autonomous Soft Robotic Fish Capable of Escape Maneuvers Using Fluidic Elastomer Actuators. *Soft Robot* **2014**, *1*, 75–87. [CrossRef]

23. Aubin, C.A.; Choudhury, S.; Jerch, R.; Archer, L.A.; Pikul, J.H.; Shepherd, R.F. Electrolytic vascular systems for energy-dense robots. *Nature* **2019**, *571*, 51–57. [CrossRef]

24. Ulloa, C.C.; Terrile, S.; Barrientos, A. Soft Underwater Robot Actuated by Shape-Memory Alloys "JellyRobcib" for Path Tracking through Fuzzy Visual Control. *Appl. Sci.* **2020**, *10*, 7160. [CrossRef]

25. Wang, Z.L.; Hang, G.R.; Li, J.A.; Wang, Y.W.; Xiao, K. A micro-robot fish with embedded SMA wire actuated flexible biomimetic fin. *Sens. Actuators A Phys.* **2008**, *144*, 354–360. [CrossRef]

26. Almubarak, Y.; Punnoose, M.; Maly, N.X.; Hamidi, A.; Tadesse, Y. KryptoJelly: A jellyfish robot with confined, adjustable pre-stress, and easily replaceable shape memory alloy NiTi actuators. *Smart Mater. Struct.* **2020**, *29*, 075011. [CrossRef]

27. Kim, D.; Gwon, M.; Kim, B.; Ortega-Jimenez, V.M.; Han, S.; Kang, D.; Bhamla, M.S.; Koh, J.-S. Design of a Biologically Inspired Water-Walking Robot Powered by Artificial Muscle. *Micromachines* **2022**, *13*, 627. [CrossRef] [PubMed]

28. Najem, J.; Sarles, S.A.; Akle, B.; Leo, D.J. Biomimetic jellyfish-inspired underwater vehicle actuated by ionic polymer metal composite actuators. *Smart Mater. Struct.* **2012**, *21*, 094026. [CrossRef]

29. Chen, Z.; Shatara, S.; Tan, X.B. Modeling of Biomimetic Robotic Fish Propelled by An Ionic Polymer-Metal Composite Caudal Fin. *IEEE ASME Trans. Mechatron.* **2010**, *15*, 448–459. [CrossRef]

30. Li, G.R.; Chen, X.P.; Zhou, F.H.; Liang, Y.M.; Xiao, Y.H.; Cao, X.; Zhang, Z.; Zhang, M.Q.; Wu, B.S.; Yin, S.Y.; et al. Self-powered soft robot in the Mariana Trench. *Nature* **2021**, *591*, 66–71. [CrossRef] [PubMed]

31. Tewary, M.; Roy, T. Dynamic analysis of dielectric elastomer membrane for actuation in soft fish robots. *J. Intell. Mater. Syst. Struct.* **2022**, *33*, 16 1045389X221085644. [CrossRef]

32. Ming, A.G.; Park, S.; Nagata, Y.; Shimojo, M. Development of Underwater Robots using Piezoelectric Fiber Composite. In Proceedings of the ICRA: 2009 IEEE International Conference on Robotics and Automation, Kobe, Japan, 12–17 May 2009; IEEE: New York, NY, USA, 2009; Volume 1–7, pp. 3435–3440.

33. Nguyen, Q.S.; Heo, S.; Park, H.C.; Goo, N.S.; Kang, T.; Voon, K.J.; Lee, S.S. A Fish Robot Driven by Piezoceramic Actuators and a Miniaturized Power Supply. *Int. J. Control Autom. Syst.* **2009**, *7*, 267–272. [CrossRef]

34. Cen, L.; Erturk, A. Bio-inspired aquatic robotics by untethered piezohydroelastic actuation. *Bioinspir. Biomim.* **2013**, *8*, 016006. [CrossRef]

35. Wang, L.; Hou, Y.J.; Zhao, K.D.; Shen, H.; Wang, Z.W.; Zhao, C.S.; Lu, X.L. A novel piezoelectric inertial rotary motor for actuating micro underwater vehicles. *Sens. Actuators A Phys.* **2019**, *295*, 428–438. [CrossRef]

36. Lou, J.; Gu, T.; Chen, T.; Yang, Y.; Xu, C.; Wei, Y.; Cui, Y. Effects of actuator-substrate ratio on hydrodynamic and propulsion performances of underwater oscillating flexible structure actuated by macro fiber composites. *Mech. Syst. Signal Process.* **2022**, *170*, 108824. [CrossRef]

37. Zhao, Q.; Chen, J.; Zhang, H.; Zhang, Z.; Liu, Z.; Liu, S.; Di, J.; He, G.; Zhao, L.; Zhang, M.; et al. Hydrodynamics Modeling of a Piezoelectric Micro-Robotic Fish With Double Caudal Fins. *J. Mech. Robot.* **2021**, *14*, 034502. [CrossRef]

38. Wehner, M.; Truby, R.L.; Fitzgerald, D.J.; Mosadegh, B.; Whitesides, G.M.; Lewis, J.A.; Wood, R.J. An integrated design and fabrication strategy for entirely soft, autonomous robots. *Nature* **2016**, *536*, 451–455. [CrossRef] [PubMed]

39. Park, S.J.; Gazzola, M.; Park, K.S.; Park, S.; Di Santo, V.; Blevins, E.L.; Lind, J.U.; Campbell, P.H.; Dauth, S.; Capulli, A.K.; et al. Phototactic guidance of a tissue-engineered soft-robotic ray. *Science* **2016**, *353*, 158–162. [CrossRef] [PubMed]

40. Nawroth, J.C.; Lee, H.; Feinberg, A.W.; Ripplinger, C.M.; McCain, M.L.; Grosberg, A.; Dabiri, J.O.; Parker, K.K. A tissue-engineered jellyfish with biomimetic propulsion. *Nat. Biotechnol.* **2012**, *30*, 792–797. [CrossRef] [PubMed]

41. Lee, K.Y.; Park, S.-J.; Matthews, D.G.; Kim, S.L.; Marquez, C.A.; Zimmerman, J.F.; Ardoña, H.A.M.; Kleber, A.G.; Lauder, G.V.; Parker, K.K. An autonomously swimming biohybrid fish designed with human cardiac biophysics. *Science* **2022**, *375*, 639–647. [CrossRef]

42. Kim, Y.; Yuk, H.; Zhao, R.K.; Chester, S.A.; Zhao, X.H. Printing ferromagnetic domains for untethered fast-transforming soft materials. *Nature* **2018**, *558*, 274–279. [CrossRef]

43. Xing, L.X.; Liao, P.; Mo, H.J.; Li, D.F.; Sun, D. Preformation Characterization of a Torque-Driven Magnetic Microswimmer with Multi-Segment Structure. *IEEE Access* **2021**, *9*, 29279–29292. [CrossRef]

44. Wang, Z.; Wang, L.; Wang, T.; Zhang, B. Research and experiments on electromagnetic-driven multi-joint bionic fish. *Robotica* **2022**, *40*, 720–746. [CrossRef]

45. Le, Q.H.; Lee, W.; Kim, Y.; Shin, B. Miniaturized double-legged robot utilizing perpendicular-axes electromagnetic actuator. *Microsyst. Technol.* **2022**, *29*, 1–10. [CrossRef]

46. Xiang, C.Q.; Guo, J.L.; Chen, Y.; Hao, L.N.; Davis, S. Development of a SMA-Fishing-Line-McKibben Bending Actuator. *IEEE Access* **2018**, *6*, 27183–27189. [CrossRef]

47. Tadesse, Y.; Villanueva, A.; Haines, C.; Novitski, D.; Baughman, R.; Priya, S. Hydrogen-fuel-powered bell segments of biomimetic jellyfish. *Smart Mater. Struct.* **2012**, *21*, 045013. [CrossRef]

48. Frame, J.; Lopez, N.; Curet, O.; Engeberg, E.D. Thrust force characterization of free-swimming soft robotic jellyfish. *Bioinspir. Biomim.* **2018**, *13*, 064001. [CrossRef] [PubMed]

49. Guan, Q.H.; Sun, J.; Liu, Y.J.; Leng, J.S. Status of and trends in soft pneumatic robotics. *Sci. Sin. Technol.* **2020**, *50*, 897–934.

50. Yirmibesoglu, O.D.; Oshiro, T.; Olson, G.; Palmer, C.; Menguc, Y. Evaluation of 3D Printed Soft Robots in Radiation Environments and Comparison With Molded Counterparts. *Front. Robot. AI* **2019**, *6*, 40. [CrossRef]

51. Yap, H.K.; Kamaldin, N.; Lim, J.H.; Nasrallah, F.A.; Goh, J.C.H.; Yeow, C.H. A Magnetic Resonance Compatible Soft Wearable Robotic Glove for Hand Rehabilitation and Brain Imaging. *IEEE Trans. Neural Syst. Rehabil. Eng.* **2017**, *25*, 782–793. [CrossRef] [PubMed]

52. Ishida, M.; Drotman, D.; Shih, B.; Hermes, M.; Luhar, M.; Tolley, M.T. Morphing Structure for Changing Hydrodynamic Characteristics of a Soft Underwater Walking Robot. *IEEE Robot. Autom. Lett.* **2019**, *4*, 4163–4169. [CrossRef]

53. Katzschmann Robert, K.; DelPreto, J.; MacCurdy, R.; Rus, D. Exploration of underwater life with an acoustically controlled soft robotic fish. *Sci. Robot.* **2018**, *3*, eaar3449. [CrossRef]

54. Calisti, M.; Picardi, G.; Laschi, C. Fundamentals of soft robot locomotion. *J. R. Soc. Interface* **2017**, *14*, 20170101. [CrossRef]

55. Katzschmann, R.K.; Marchese, A.D.; Rus, D. Hydraulic Autonomous Soft Robotic Fish for 3D Swimming. In *Experimental Robotics: The 14th International Symposium on Experimental Robotics*; Hsieh, M.A., Khatib, O., Kumar, V., Eds.; Springer International Publishing: Berlin/Heidelberg, Germany, 2016; pp. 405–420.

56. Joshi, A.; Kulkarni, A.; Tadesse, Y. FludoJelly: Experimental Study on Jellyfish-Like Soft Robot Enabled by Soft Pneumatic Composite (SPC). *Robotics* **2019**, *8*, 56. [CrossRef]

57. Fan, J.; Wang, S.; Yu, Q.; Zhu, Y. Experimental Study on Frog-inspired Swimming Robot Based on Articulated Pneumatic Soft Actuator. *J. Bionic Eng.* **2020**, *17*, 270–280. [CrossRef]

58. Belter, D.; Skrzypczyński, P. Rough terrain mapping and classification for foothold selection in a walking robot. *J. Field Robot.* **2011**, *28*, 497–528. [CrossRef]

59. Chu, W.S.; Lee, K.T.; Song, S.H.; Han, M.W.; Lee, J.Y.; Kim, H.S.; Kim, M.S.; Park, Y.J.; Cho, K.J.; Ahn, S.H. Review of biomimetic underwater robots using smart actuators. *Int. J. Precis. Eng. Manuf.* **2012**, *13*, 1281–1292. [CrossRef]

60. Kwak, B.; Bae, J. Locomotion of arthropods in aquatic environment and their applications in robotics. *Bioinspir. Biomim.* **2018**, *13*, 041002. [CrossRef] [PubMed]

61. Hou, T.G.; Yang, X.B.; Su, H.H.; Jiang, B.H.; Chen, L.K.; Wang, T.M.; Liang, J.H. Design and Experiments of a Squid-like Aquatic-aerial Vehicle with Soft Morphing Fins and Arms. In Proceedings of the 2019 International Conference on Robotics and Automation, Montreal, QC, Canada, 20–24 May 2019; Howard, A., Althoefer, K., Arai, F., Arrichiello, F., Caputo, B., Castellanos, J., Hauser, K., Isler, V., Kim, J., Liu, H., et al., Eds.; IEEE: New York, NY, USA, 2019; pp. 4681–4687.

62. Chou, C.P.; Hannaford, B. Measurement and modeling of McKibben pneumatic artificial muscles. *IEEE Trans. Robot. Autom.* **1996**, *12*, 90–102. [CrossRef]

63. Tondu, B. Modelling of the McKibben artificial muscle: A review. *J. Intell. Mater. Syst. Struct.* **2012**, *23*, 225–253. [CrossRef]

64. Guan, Q.H.; Sun, J.; Liu, Y.J.; Wereley, N.M.; Leng, J.S. Novel Bending and Helical Extensile/Contractile Pneumatic Artificial Muscles Inspired by Elephant Trunk. *Soft Robot.* **2020**, *7*, 597–614. [CrossRef]
65. Pillsbury, T.E.; Wereley, N.M.; Guan, Q.H. Comparison of contractile and extensile pneumatic artificial muscles. *Smart Mater. Struct.* **2017**, *26*, 095034. [CrossRef]
66. Bishop-Moser, J.; Krishnan, G.; Kim, C.; Kota, S. Kinematic Synthesis of Fiber Reinforced Soft Actuators in Paralell Combinations. In Proceedings of the ASME 2012 International Design Engineering Technical Conferences and Computers and Information in Engineering Conference, Chicago, IL, USA, 12–12 August 2012; pp. 1079–1087.
67. Suzumori, K.; Iikura, S.; Tanaka, H. Flexible Microactuator for Miniature Robots. In Proceedings of the IEEE International Conference on Micro Electro Mechanical Systems, Nara, Japan, 30–32 January 1991; IEEE: New York, NY, USA, 1991; pp. 204–209.
68. Bishop-Moser, J.; Krishnan, G.; Kim, C.; Kota, S. Design of Soft Robotic Actuators using Fluid-filled Fiber-Reinforced Elastomeric Enclosures in Parallel Combinations. In Proceedings of the 2012 IEEE/RSJ International Conference on Intelligent Robots and Systems, Ilamoura-Algarve, Portugal, 7–12 October 2012; pp. 4264–4269.
69. Ilievski, F.; Mazzeo, A.D.; Shepherd, R.F.; Chen, X.; Whitesides, G.M. Soft Robotics for Chemists. *Angew. Chem. Int. Ed.* **2011**, *50*, 1890–1895. [CrossRef]
70. Mosadegh, B.; Polygerinos, P.; Keplinger, C.; Wennstedt, S.; Shepherd, R.F.; Gupta, U.; Shim, J.; Bertoldi, K.; Walsh, C.J.; Whitesides, G.M. Pneumatic Networks for Soft Robotics that Actuate Rapidly. *Adv. Funct. Mater.* **2014**, *24*, 2163–2170. [CrossRef]
71. Katzschmann, R.K.; Marchese, A.D.; Rus, D. Autonomous Object Manipulation Using a Soft Planar Grasping Manipulator. *Soft Robot.* **2015**, *2*, 155–164. [CrossRef] [PubMed]
72. Wang, Z.K.; Zhu, M.Z.; Kawamura, S.; Hirai, S. Comparison of different soft grippers for lunch box packaging. *Robot. Biomim.* **2017**, *4*, 9. [CrossRef] [PubMed]
73. Hao, Y.F.; Gong, Z.Y.; Xie, Z.X.; Guan, S.Y.; Yang, X.B.; Ren, Z.Y.; Wang, T.M.; Wen, L. Universal soft pneumatic robotic gripper with variable effective length. In Proceedings of the 35th Chinese Control Conference 2016, Chengdu, China, 27–29 July 2016; Chen, J., Zhao, Q., Eds.; IEEE: New York, NY, USA, 2016; pp. 6109–6114.
74. Chi, Y.; Tang, Y.; Liu, H.; Yin, J. Leveraging Monostable and Bistable Pre-Curved Bilayer Actuators for High-Performance Multitask Soft Robots. *Adv. Mater. Technol.* **2020**, *5*, 2000370. [CrossRef]
75. Tang, Y.; Chi, Y.; Sun, J.; Huang, T.-H.; Maghsoudi, O.H.; Spence, A.; Zhao, J.; Su, H.; Yin, J. Leveraging elastic instabilities for amplified performance: Spine-inspired high-speed and high-force soft robots. *Sci. Adv.* **2020**, *6*. [CrossRef]
76. Yang, D.; Mosadegh, B.; Ainla, A.; Lee, B.; Khashai, F.; Suo, Z.; Bertoldi, K.; Whitesides, G.M. Buckling of Elastomeric Beams Enables Actuation of Soft Machines. *Adv. Mater.* **2015**, *27*, 6323–6327. [CrossRef]
77. Yang, D.; Verma, M.S.; So, J.H.; Mosadegh, B.; Keplinger, C.; Lee, B.; Khashai, F.; Lossner, E.; Suo, Z.G.; Whitesides, G.M. Buckling Pneumatic Linear Actuators Inspired by Muscle. *Adv. Mater. Technol.* **2016**, *1*, 1600055. [CrossRef]
78. Jiao, Z.D.; Ji, C.; Zou, J.; Yang, H.Y.; Pan, M. Vacuum-Powered Soft Pneumatic Twisting Actuators to Empower New Capabilities for Soft Robots. *Adv. Mater. Technol.* **2019**, *4*, 1800429. [CrossRef]
79. Ainla, A.; Verma, M.S.; Yang, D.; Whitesides, G.M. Soft, Rotating Pneumatic Actuator. *Soft Robot.* **2017**, *4*, 297–304. [CrossRef]
80. Lee, J.G.; Rodrigue, H. Origami-Based Vacuum Pneumatic Artificial Muscles with Large Contraction Ratios. *Soft Robot.* **2019**, *6*, 109–117. [CrossRef]
81. Shepherd, R.F.; Stokes, A.A.; Freake, J.; Barber, J.; Snyder, P.W.; Mazzeo, A.D.; Cademartiri, L.; Morin, S.A.; Whitesides, G.M. Using Explosions to Power a Soft Robot. *Angew. Chem.* **2013**, *125*, 2964–2968. [CrossRef]
82. Bartlett, N.W.; Tolley, M.T.; Overvelde, J.T.B.; Weaver, J.C.; Mosadegh, B.; Bertoldi, K.; Whitesides, G.M.; Wood, R.J. A 3D-printed, functionally graded soft robot powered by combustion. *Science* **2015**, *349*, 161–165. [CrossRef] [PubMed]
83. Suzumori, K.; Endo, S.; Kanda, T.; Kato, N.; Suzuki, H. A Bending Pneumatic Rubber Actuator Realizing Soft-bodied Manta Swimming Robot. In Proceedings of the 2007 IEEE International Conference on Robotics and Automation, Roma, Italy, 10–14 April 2007; pp. 4975–4980.
84. Feng, H.; Sun, Y.; Todd, P.A.; Lee, H.P. Body Wave Generation for Anguilliform Locomotion Using a Fiber-Reinforced Soft Fluidic Elastomer Actuator Array Toward the Development of the Eel-Inspired Underwater Soft Robot. *Soft Robot.* **2019**, *7*, 233–250. [CrossRef] [PubMed]
85. Cai, Y.; Bi, S.; Zheng, L. Design and Experiments of a Robotic Fish Imitating Cow-Nosed Ray. *J. Bionic Eng.* **2010**, *7*, 120–126. [CrossRef]
86. Zhang, Z.; Philen, M.; Neu, W. Development of a Bio-Inspired Artificial Fish Using Flexible Matrix Composite Actuators. In Proceedings of the ASME 2009 Conference on Smart Materials, Adaptive Structures and Intelligent Systems, Oxnard, CA, USA, 21–23 September 2009; pp. 621–630.
87. Zhang, Z.; Philen, M.; Neu, W. A biologically inspired artificial fish using flexible matrix composite actuators: Analysis and experiment. *Smart Mater. Struct.* **2010**, *19*, 094017. [CrossRef]
88. Fan, J.-Z.; Zhang, W.; Kong, P.-C.; Cai, H.-G.; Liu, G.-F. Design and Dynamic Model of a Frog-inspired Swimming Robot Powered by Pneumatic Muscles. *Chin. J. Mech. Eng.* **2017**, *30*, 1123–1132. [CrossRef]
89. Anderson, J.M.; Chhabra, N.K. Maneuvering and Stability Performance of a Robotic Tuna1. *Integr. Comp. Biol.* **2002**, *42*, 118–126. [CrossRef]
90. Nguyen, D.Q.; Ho, V.A. Kinematic Evaluation of a Series of Soft Actuators in Designing an Eel-inspired Robot. In Proceedings of the 2020 IEEE/SICE International Symposium on System Integration (SII), Honolulu, HI, USA, 12–15 January 2020; pp. 1288–1293.

91. Yinding, C.; Yaoye, H.; Yao, Z.; Yanbin, L.; Jie, Y. Snapping for high-speed and high-efficient, butterfly swimming-like soft flapping-wing robot. *arXiv* **2022**, arXiv:2204.05987.

92. Li, Y.; Fish, F.; Chen, Y.; Ren, T.; Zhou, J. Bio-inspired robotic dog paddling: Kinematic and hydro-dynamic analysis. *Bioinspir. Biomim.* **2019**, *14*, 066008. [CrossRef]

93. Fan, J.Z.; Du, Q.L.; Yu, Q.G.; Wang, Y.; Qi, J.M.; Zhu, Y.H. Biologically inspired swimming robotic frog based on pneumatic soft actuators. *Bioinspir. Biomim.* **2020**, *15*, 046006. [CrossRef]

94. Nemiroski, A.; Shevchenko, Y.Y.; Stokes, A.A.; Unal, B.; Ainla, A.; Albert, S.; Compton, G.; MacDonald, E.; Schwab, Y.; Zellhofer, C.; et al. Arthrobots. *Soft Robot.* **2017**, *4*, 183–190. [CrossRef] [PubMed]

95. Cheng, P.; Ye, Y.; Jia, J.; Wu, C.; Xie, Q. Design of cylindrical soft vacuum actuator for soft robots. *Smart Mater. Struct.* **2021**, *30*, 045020. [CrossRef]

96. Keithly, D.; Whitehead, J.; Voinea, A.; Horna, D.; Hollenberg, S.; Peck, M.; Pikul, J.; Shepherd, R.F. A cephalopod-inspired combustion powered hydro-jet engine using soft actuators. *Extrem. Mech. Lett.* **2018**, *20*, 1–8. [CrossRef]

97. Zufferey, R.; Siddall, R.; Armanini, S.F.; Kovac, M. Aquatic Escape: Repeatable Escape with Combustion. In *Between Sea and Sky: Aerial Aquatic Locomotion in Miniature Robots*; Zufferey, R., Siddall, R., Armanini, S.F., Kovac, M., Eds.; Springer International Publishing: Berlin/Heidelberg, Germany, 2022; pp. 131–153.

98. Nagarkar, A.; Lee, W.-K.; Preston Daniel, J.; Nemitz Markus, P.; Deng, N.-N.; Whitesides George, M.; Mahadevan, L. Elastic-instability–enabled locomotion. *Proc. Natl. Acad. Sci. USA* **2021**, *118*, e2013801118. [CrossRef] [PubMed]

99. Polygerinos, P.; Wang, Z.; Overvelde, J.T.B.; Galloway, K.C.; Wood, R.J.; Bertoldi, K.; Walsh, C.J. Modeling of Soft Fiber-Reinforced Bending Actuators. *IEEE Trans. Robot.* **2015**, *31*, 778–789. [CrossRef]

100. Galloway, K.C.; Polygerinos, P.; Walsh, C.J.; Wood, R.J. Mechanically Programmable Bend Radius for Fiber-Reinforced Soft Actuators. In Proceedings of the 2013 16th International Conference on Advanced Robotics (ICAR), Montevideo, Uruguay, 25–29 November 2013; IEEE: New York, NY, USA, 2013.

101. Liu, T.-Y.; Li, D.-D.; Ye, J.; Li, Q.; Sheng, L.; Liu, J. An Integrated Soft Jumping Robotic Module Based on Liquid Metals. *Adv. Eng. Mater.* **2021**, *23*, 2100515. [CrossRef]

102. Tolley, M.T.; Shepherd, R.F.; Karpelson, M.; Bartlett, N.W.; Galloway, K.C.; Wehner, M.; Nunes, R.; Whitesides, G.M.; Wood, R.J. An untethered jumping soft robot. In Proceedings of the 2014 IEEE/RSJ International Conference on Intelligent Robots and Systems, Chicago, IL USA, 14–18 September 2014; pp. 561–566.

103. Drucker, E.G.; Lauder, G.V. Locomotor forces on a swimming fish: Three-dimensional vortex wake dynamics quantified using digital particle image velocimetry. *J. Exp. Biol.* **1999**, *202*, 2393–2412. [CrossRef]

104. Kikuchi, K.; Uehara, Y.; Kubota, Y.; Mochizuki, O. Morphological Considerations of Fish Fin Shape on Thrust Generation. *J. Appl. Fluid Mech.* **2014**, *7*, 625–632.

105. Feilich, K.L.; Lauder, G.V. Passive mechanical models of fish caudal fins: Effects of shape and stiffness on self-propulsion. *Bioinspir. Biomim.* **2015**, *10*, 036002. [CrossRef]

106. Wen, L.; Wang, T.M.; Wu, G.H.; Liang, J.H. Quantitative Thrust Efficiency of a Self-Propulsive Robotic Fish: Experimental Method and Hydrodynamic Investigation. *IEEE-ASME Trans. Mechatron.* **2013**, *18*, 1027–1038. [CrossRef]

107. Cheng, J.Y.; Davison, I.G.; DeMont, M.E. Dynamics and energetics of scallop locomotion. *J. Exp. Biol.* **1996**, *199*, 1931–1946. [CrossRef] [PubMed]

108. Rogers, E.; Polygerinos, P.; Walsh, C.; Goldfield, E. Smart and Connected Actuated Mobile and Sensing Suit to Encourage Motion in Developmentally Delayed Infants1. *J. Med. Devices* **2015**, *9*, 1027–1038. [CrossRef]